



# Magnetic ordering in $\text{TlFe}_{1.3}\text{Se}_2$ studied by Mössbauer spectroscopy

Zbigniew M. Stadnik<sup>a,\*</sup>, Pu Wang<sup>b</sup>, Hang-Dong Wang<sup>c,d</sup>, Chi-Heng Dong<sup>c</sup>, Ming-Hu Fang<sup>c</sup>

<sup>a</sup> Department of Physics, University of Ottawa, Ottawa, Ontario, Canada K1N 6N5

<sup>b</sup> Key Laboratory of Extreme Conditions Physics, The Institute of Physics, Chinese Academy of Sciences, Beijing 100190, China

<sup>c</sup> Department of Physics, Zhejiang University, Hangzhou 310027, China

<sup>d</sup> Department of Physics, Hangzhou Normal University, Hangzhou 310036, China

## ARTICLE INFO

### Article history:

Received 19 December 2012

Received in revised form 16 January 2013

Accepted 17 January 2013

Available online 4 February 2013

### Keywords:

Antiferromagnetism

Phase separation

Mössbauer spectroscopy

## ABSTRACT

We report the results of  $^{57}\text{Fe}$  Mössbauer spectroscopy measurements of the new nonsuperconducting compound  $\text{TlFe}_{1.3}\text{Se}_2$  in the temperature range 4.4–373.2 K and in an external magnetic field of 90 kOe. We provide evidence for a possible phase separation into magnetic majority and minority phases. We show that these magnetic phases order antiferromagnetically with two different magnetic moments at 5.0 K of 2.00(1) and 1.40(2)  $\mu_B$ , and with the Néel temperature  $T_N = 324.5(6.3)$  K. We find that the Debye temperature of the studied compound is 221(2) K.

© 2013 Elsevier B.V. All rights reserved.

## 1. Introduction

Recently, there has been renewed interest in the family of Fe-deficient compounds  $\text{TlFe}_{2-y}\text{Se}_2$  that had been synthesized and studied a long time ago [1–4]. This interest has been triggered by the discovery of superconductivity in iron-based superconductors [5–7]. In particular, the recent discovery of superconductivity in iron-selenide compounds  $A_x\text{Fe}_{2-y}\text{Se}_2$  and  $(A,\text{Tl})_x\text{Fe}_{2-y}\text{Se}_2$  ( $A = \text{K}, \text{Rb}, \text{Cs}$ ) [8–14], with critical temperatures up to about 32 K, has resulted in a renewed interest in iron-based chalcogenide compounds.

Initially, these new superconductors were believed to have the crystal structure of the  $\text{ThCr}_2\text{Si}_2$  type (space group  $I4/mmm$ ) [15], but it was soon realized that there is a well-defined  $\sqrt{5} \times \sqrt{5} \times 1$  ordering of Fe vacancies, similarly to what had been proposed by Häggström et al. [2] for  $\text{TlFe}_{2-y}\text{Se}_2$  compounds, which reduces the symmetry to the space group  $I4/m$  [16–18]. A remarkable characteristic of these new superconductors is that they are very strong antiferromagnets, with unprecedentedly high values of Néel temperature,  $T_N$ , of 475–559 K (Refs. [17,19–23]) and of Fe magnetic moment of 2.0–3.3  $\mu_B$  [17,22,24–26]. Although it is still under debate how superconductivity can coexist with such strong antiferromagnetism in these superconductors, there is an increasing body of experimental evidence [27] suggesting that the antiferromagnetic phase is spatially separated from the superconducting phase.

In view of this renewed interest in the  $\text{TlFe}_{2-y}\text{Se}_2$  compounds [28–31], we have carried out a detailed study of the recently synthesized new compound  $\text{TlFe}_{1.3}\text{Se}_2$  (Ref. [14]) with Mössbauer spectroscopy. We provide evidence for a possible separation into magnetic majority and minority phases. We show that the compound studied is an antiferromagnet with  $T_N = 324.5(6.3)$  K.

## 2. Experimental methods

The single crystals of the studied compound  $\text{TlFe}_{1.3}\text{Se}_2$  were grown by the Bridgeman method [14]. Powder X-ray diffraction measurements were performed at 298 K in Bragg–Brentano geometry with a PANalytical X'Pert scanning diffractometer using  $\text{Cu K}\alpha$  radiation.

The  $^{57}\text{Fe}$  Mössbauer measurements were conducted using standard Mössbauer spectrometers operating in sine mode and a 100-mCi  $^{57}\text{Co}(\text{Rh})$  source, which was kept at the same temperature as that of the absorber for in-field measurements and at room temperature for zero-field measurements. The spectrometers used for zero-field and in-field measurements were calibrated, respectively, with a 6.35- $\mu\text{m}$ -thick  $\alpha\text{-Fe}$  foil [32] and a Michelson interferometer [33], and the spectra were folded.

The Mössbauer absorber for low-temperature (<300 K) measurements was made in a glove box from several pulverized single crystals. The powder material was mixed with boron nitride and was put into a high-purity, 8- $\mu\text{m}$ -thick Al disk container to ensure a uniform temperature over the whole absorber. The Mössbauer absorber for high-temperature measurements (>300 K) was made in a glove box from several pulverized single crystals. The powder material was mixed with boron nitride and placed into a boron-nitride container. The surface densities of the Mössbauer absorbers for low-temperature and high-temperature measurements were 24.3  $\text{mg}/\text{cm}^2$  and 17.5  $\text{mg}/\text{cm}^2$ , respectively. Both Mössbauer absorbers were exposed to air for about 60 s when they were transported from the glove box to the Mössbauer cryostat and the Mössbauer oven. The high atomic absorption of the 14.4-keV  $\gamma$ -rays by Tl and Se, and a relatively small concentration of Fe in the compound studied, necessitated an acquisition time of about 3–7 days for a single Mössbauer spectrum.

\* Corresponding author. Tel.: +1 6135625800.

E-mail address: [stadnik@uottawa.ca](mailto:stadnik@uottawa.ca) (Z.M. Stadnik).

The surface densities of the Mössbauer absorbers for low-temperature and high-temperature measurements correspond to an effective thickness parameter [34]  $T$  of  $2.4f_a$  and  $1.7f_a$ , respectively, where  $f_a$  is the Lamb-Mössbauer factor of the absorber. Since  $T > 1$ , the resonance line shape of the Mössbauer spectrum was described using a transmission integral formula [35]. In addition to the hyperfine parameters, only the absorber Debye–Waller factor  $f_a$  and the absorber linewidth  $\Gamma_a$  were fitted as independent parameters. The source linewidth  $\Gamma_s = 0.130$  mm/s and the background-corrected Debye–Waller factor of the source  $f_s = 0.30$  were used in the fits [35]. The  $^{57}\text{Fe}$  Mössbauer spectra were analyzed by means of a least-squares fitting procedure which entailed calculations of the positions and relative intensities of the absorption lines by numerical diagonalization of the full hyperfine interaction Hamiltonian [34].

### 3. Experimental results and discussion

The room-temperature powder  $x$ -ray diffraction pattern of  $\text{TlFe}_{1.3}\text{Se}_2$  is shown in Fig. 1. It reveals that the studied compound is single phase as there are no extrinsic Bragg peaks present in the measured pattern. The structural parameters of  $\text{TlFe}_{1.3}\text{Se}_2$  obtained from the Rietveld refinement (Fig. 1) in the  $I4/mmm$  space group are listed in Table 1. Rietveld analysis of the powder  $x$ -ray diffraction pattern of  $\text{TlFe}_{1.3}\text{Se}_2$ , with a freely refined occupancy (Table 1) of Fe [0.727(23)], yields the formula  $\text{TlFe}_{1.45}\text{Se}_2$  for the compound of nominal composition  $\text{TlFe}_{1.3}\text{Se}_2$ .

The  $^{57}\text{Fe}$  Mössbauer spectra of  $\text{TlFe}_{1.3}\text{Se}_2$  at 5.0 K measured in the external magnetic fields  $H_{\text{ext}} = 0$  and 90 kOe applied parallel to the  $\gamma$ -ray propagation direction are shown in Fig. 2. One can see that the zero-field spectrum (Fig. 2) results from the superposition of at least two Zeeman patterns. The fit of this spectrum with two Zeeman patterns yields the following parameters: the absorber linewidth  $\Gamma_a$ , the centre shift  $\delta$  (relative to  $\alpha$ -Fe at 298 K), the hyperfine magnetic fields  $H$ , the quadrupole splitting  $\Delta = \frac{1}{2}eQV_{zz}$  (where  $e$  is the proton charge,  $Q$  is the electric quadrupole moment of the  $^{57}\text{Fe}$  nucleus [36], and  $V_{zz}$  is the principal component of the electric field gradient tensor), the asymmetry parameter  $\eta$ , the angle  $\beta$  between  $V_{zz}$  and  $H$ , and the spectral area  $A$  [34]. The values of these parameters corresponding to these two-component Zeeman patterns are  $\Gamma_{a1} = 0.179(13)$  mm/s,  $\Gamma_{a2} = 0.207(40)$  mm/s,  $\delta_1 = 0.541(4)$  mm/s,  $\delta_2 = 0.445(19)$  mm/s,  $H_1 = 268.3(1.8)$  kOe,  $H_2 = 187.4(2.5)$  kOe,  $\Delta_1 = 0.946(179)$  mm/s,  $\Delta_2 = 1.837(94)$  mm/s,  $\eta_1 = 0.1(2)$ ,  $\eta_2 = 0.0(2)$ ,  $\beta_1 = 44(6)^\circ$ ,  $\beta_2 = 48(1)^\circ$ ,  $A_1 = 75.7(7)\%$ ,  $A_2 = 24.3(9)\%$ .

As the Fe atoms are located at the  $4d$  sites in the space group  $I4/mmm$  (Table 1), one would expect to observe at temperatures below the magnetic ordering temperature one Zeeman pattern, and not two (Fig. 2). A question then arises as to the origin of the minority Zeeman pattern observed experimentally. Following the

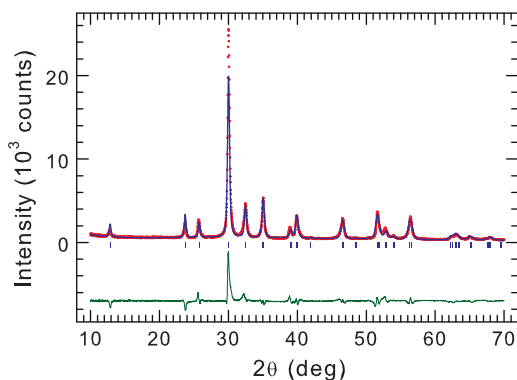


**Fig. 1.** The powder  $x$ -ray diffraction pattern of  $\text{TlFe}_{1.3}\text{Se}_2$  at 298 K. The experimental data are denoted by open circles, while the line through the circles represents the result of the Rietveld refinement. The row of vertical bars shows the Bragg peak positions for the  $I4/mmm$  space group. The lower solid line represents the difference curve between experimental and calculated patterns.

**Table 1**

Refined structural parameters of  $\text{TlFe}_{1.3}\text{Se}_2$  at 298 K. Space group:  $I4/mmm$  (No. 139), lattice constants  $a = 3.9047(3)$  Å,  $c = 13.8634(6)$  Å.

Atom	Site	Point symmetry	Occupancy	x	y	z	$B_{\text{iso}}$ (Å <sup>2</sup> )
Tl	2a	4/mmm	1.0	0	0	0	1.6(1)
Fe	4d	4m2	0.727(23)	0	$\frac{1}{2}$	$\frac{1}{4}$	0.5(1)
Se	4e	4mm	1.0	0	0	0.353(3)	1.1(2)

$R_p = 11.9\%$ ,  $R_{wp} = 15.3\%$ ,  $\chi^2 = 18.4$

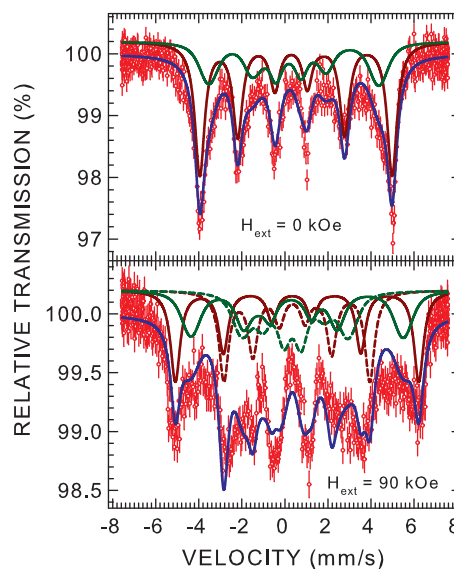


**Fig. 2.** The  $^{57}\text{Fe}$  Mössbauer spectra of  $\text{TlFe}_{1.3}\text{Se}_2$  at 5.0 K in zero and 90 kOe external magnetic field  $H_{\text{ext}}$  applied parallel to the direction of the  $\gamma$ -rays, fitted (blue solid lines) with two Zeeman patterns (brown and green lines), as described in the text. The zero-velocity origin is relative to the source. (For interpretation of the references to color in this figure legend, the reader is referred to the web version of this article.)

analysis of Mössbauer spectra of isotypic  $\text{TlFe}_{2-y}\text{S}_2$  compounds [37], it could be argued that the two Zeeman patterns observed are due to Fe atoms with nearest-neighbor configurations of two and three Fe atoms. For the compound studied, the probabilities of such configurations, which are proportional to the spectral areas of the corresponding Zeeman patterns, are 31% and 38%, respectively. The predicted ratio of the spectral areas 31:38 is completely different from the observed ratio 75.7:24.3, and thus the interpretation of the origin of the component Zeeman patterns as being due to different nearest-neighbor configurations of Fe atoms [37] is not applicable here. We propose that the minority Zeeman pattern arises from a separated nanoscale phase of regions with disordered Fe vacancies. This proposition is based upon recent observations in the nonsuperconducting compound  $\text{TlFe}_{1.6}\text{Se}_2$  (Ref. [31]) by means of atomic-resolution  $Z$ -contrast scanning transmission electron microscopy which find of the phase separation into two regions having the same composition, of Fe vacancy order and disorder. We note here that phase separation has been observed with different experimental techniques in  $(\text{Tl,Rb})_x\text{Fe}_{2-y}\text{Se}_2$  (Refs. [38,39]),  $\text{Tl}_{0.5}\text{K}_{0.3}\text{Fe}_{1.6}\text{Se}_2$  (Ref. [39]), and  $\text{Tl}_{0.75}\text{K}_{0.25}\text{Fe}_{1.86}\text{Se}_2$  (Ref. [27]) superconductors, and in nonsuperconducting  $\text{Tl}_{0.53}\text{K}_{0.47}\text{Fe}_{1.64}\text{Se}_2$  (Ref. [30]) and  $\text{TlFe}_{1.6}\text{Se}_2$  [31]. It thus appears that phase separation is commonly observed in the  $\text{TlFe}_{2-y}\text{Se}_2$  system.

The relatively large values of  $\delta$  indicate that Fe atoms in both the main and separated magnetic phases are in the divalent oxidation state [34]. One can estimate the on-site magnetic moment  $\mu$  of iron atoms from the measured  $H$  since, to a first approximation,  $H$

is proportional to  $\mu$  via the relation  $H = a\mu$ , where the value of the proportionality constant  $a$  is compound specific [40]. To convert  $H$  to  $\mu$ ,  $a = 134 \text{ kOe}/\mu_B$  was used. This value of  $a$  was obtained from  $H(4.2 \text{ K}) = 201(4) \text{ kOe}$  and  $\mu(16 \text{ K}) = 1.5(2)\mu_B$  determined from a Mössbauer and neutron diffraction study of orthorhombic  $\text{Ti}_3\text{Fe}_2\text{S}_4$  [41]. Thus, the values of the iron magnetic moments at 5.0 K of the majority and the minority phases are 2.00(1) and 1.40(2)  $\mu_B$ , respectively.

The  $^{57}\text{Fe}$  Mössbauer spectra of a magnetically ordered compound measured in zero external magnetic field give information on the magnitude and direction of the hyperfine magnetic field, and thus of the Fe magnetic moment, but not on the type of magnetic ordering of these moments. Information on the type of magnetic ordering can be obtained from Mössbauer spectra measured in a strong enough external magnetic field  $H_{\text{ext}}$  [42]. It can be observed in the Mössbauer spectrum of  $\text{TiFe}_{1.3}\text{Se}_2$  measured in  $H_{\text{ext}} = 90 \text{ kOe}$  (Fig. 2) that each component Zeeman pattern in the zero-field spectrum is split into two components of equal intensity. Furthermore, the fitted hyperfine magnetic fields  $H_i(H_{\text{ext}})$  ( $i = 1, 2$ )

obey, within experimental error, the relation  $H_i(H_{\text{ext}}) = H_i \pm H_{\text{ext}}$  ( $i = 1, 2$ ). This clearly demonstrates [42,43] the antiferromagnetic ordering of the Fe magnetic moments in the compound studied. In addition, obeying this relation means that the spin-flop field [42,43] for the studied antiferromagnet is larger than 90 kOe.

Fig. 3 shows the  $^{57}\text{Fe}$  Mössbauer spectra of  $\text{TiFe}_{1.3}\text{Se}_2$  measured in the temperature range 4.4–373.2 K. The spectra at 4.4 and 34.9 K can be fitted with two Zeeman patterns, similarly to the zero-field spectrum at 5.0 K in Fig. 2. However, the fits of the spectra at 48.4 K and at higher temperatures (Fig. 3) require the inclusion of an additional quadrupole doublet pattern. The spectral area of this quadrupole doublet pattern increases with temperature at the expense of the spectral area of the two Zeeman patterns. What is also evident from visual inspection of the spectra in Fig. 3 is that the hyperfine magnetic fields  $H_1$  and  $H_2$  corresponding to the two Zeeman patterns decrease with temperature, as expected, but that this decrease is unusually small. This can be clearly seen in Fig. 4 which shows the temperature dependence of  $H_1$  and  $H_2$  derived from the fits of the Mössbauer spectra in Figs. 2 and 3.

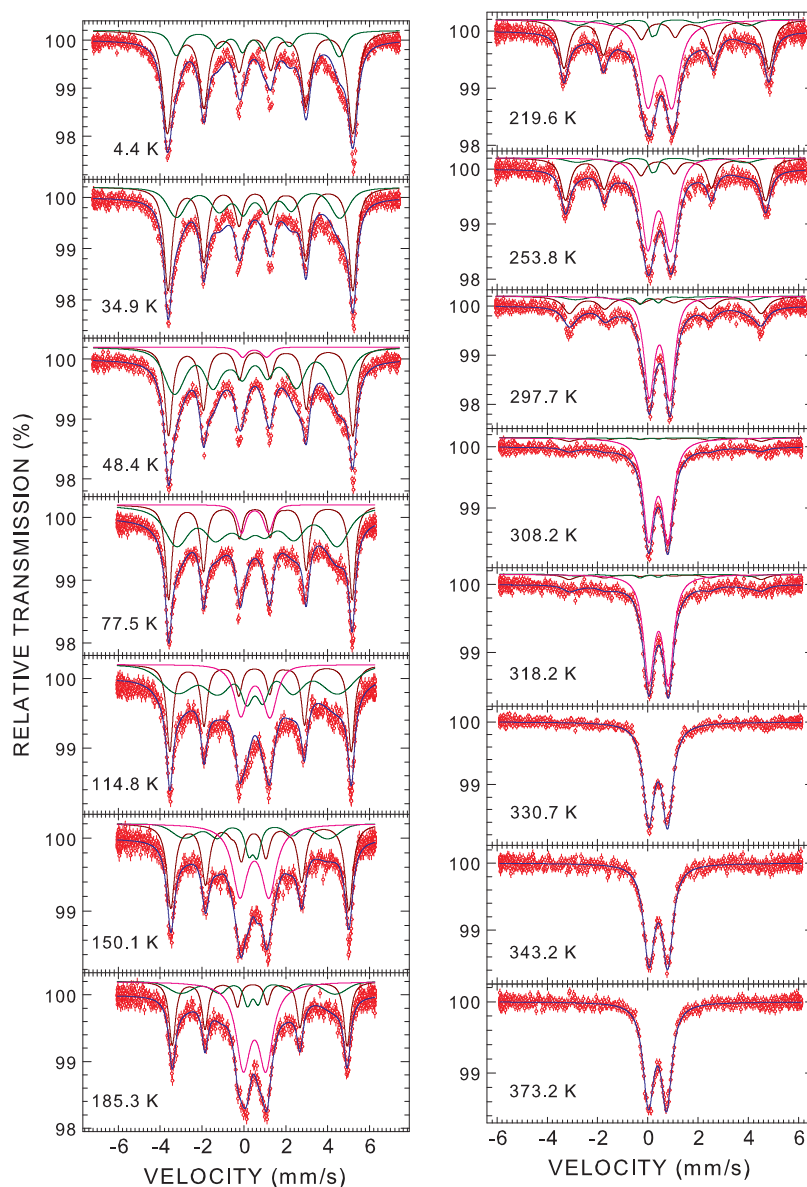


**Fig. 3.** The  $^{57}\text{Fe}$  Mössbauer spectra of  $\text{TiFe}_{1.3}\text{Se}_2$  at the indicated temperatures fitted (blue solid lines) with two Zeeman patterns (brown and green solid lines) and a quadrupole doublet pattern (pink solid lines), as described in the text. The zero-velocity origin is relative to  $\alpha$ -Fe at room temperature. (For interpretation of the references to color in this figure legend, the reader is referred to the web version of this article.)

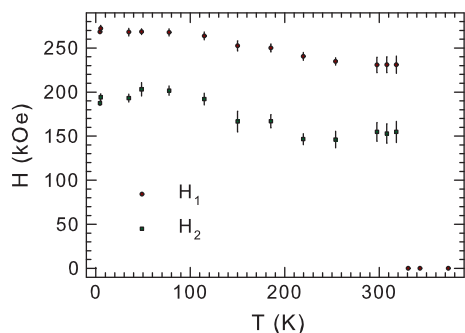


**Fig. 4.** The temperature dependence of the hyperfine magnetic fields  $H_1$  and  $H_2$  determined from the fits of the spectra in Figs. 2 and 3. The experimental points at 330.7, 343.2 and 373.2 K correspond to  $H_1 = H_2 = 0$ .

One observes a sudden drop of the hyperfine magnetic field (Fig. 4) at  $T_N = 324.5(6.3)$  K: at 318.2 K  $H_1 \neq 0$  and  $H_2 \neq 0$ , but at 330.7 K  $H_1 = H_2 = 0$ . Clearly, the transition at  $T_N = 324.5(6.3)$  K is a first order magnetic transition. A similar abrupt drop of the hyperfine magnetic field around  $T_N$  was observed for the nonsuperconducting compounds  $\text{TlFe}_{2-y}\text{Se}_2$  ( $y = 0.36, 0.38, 0.39$  and  $0.40$ ) [2–4]. The observation of a common Néel temperature for the ordered and disordered magnetic phases suggests that they are somehow intertwined at the nanoscale.

The temperature dependence of the quadrupole splitting  $\Delta_3$  corresponding to a quadrupole doublet pattern, as determined from the fits of the spectra in Fig. 3, is displayed in Fig. 5. One can observe a clear increase in  $\Delta_3$  with decreasing temperature. This experimental  $\Delta_3(T)$  dependence can be fitted to the empirical equation

$$\Delta_3(T) = \Delta_3(0)(1 - BT^{3/2}), \quad (1)$$

where  $\Delta_3(0)$  is the value of  $\Delta_3$  at 0 K and  $B$  is a constant. Such a  $T^{3/2}$  temperature dependence has been observed in many metallic non-cubic compounds [44]. This apparently universal  $T^{3/2}$  dependence is not well understood. Its origin seems to be associated with a strong temperature dependence of mean-square lattice displacements and, to a lesser extent, with the temperature dependence of the lattice parameters [45]. The values of  $\Delta_3(0)$  and  $B$  determined from the fit are, respectively,  $1.226(43)$  mm/s and  $6.27(47) \times 10^{-5} \text{ K}^{-3/2}$ . We note that the values of  $\Delta_3(0)$  and  $B$  found here are very close to the corresponding values found for the nonsuperconducting compounds  $\text{TlFe}_{2-y}\text{Se}_2$  ( $y = 0.38, 0.39$  and  $0.40$ ) [4].

The absorption spectral area  $A$  of a Mössbauer spectrum is proportional to the absorber Debye–Waller factor  $f_a$  given [34] by

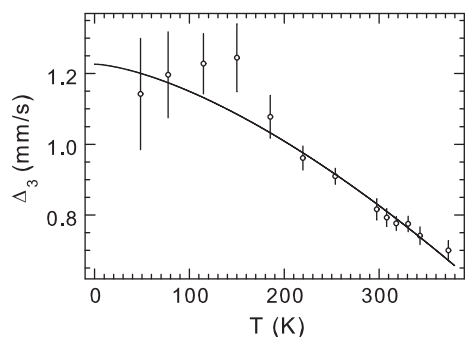


**Fig. 5.** The temperature dependence of the quadrupole splitting  $\Delta_3$  corresponding to a quadrupole doublet pattern in Fig. 3. The solid line is the fit to Eq. (1), as explained in the text.

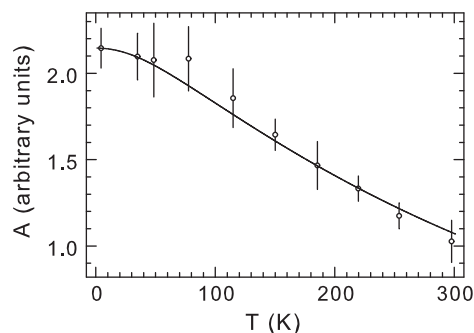


**Fig. 6.** The temperature dependence of the absorption spectral area  $A$ . The solid line is the fit to Eq. (2), as explained in the text.

$$f_a(T) = \exp \left\{ -\frac{3}{4} \frac{E_\gamma^2}{Mc^2 k_B \Theta_D} \left[ 1 + 4 \left( \frac{T}{\Theta_D} \right)^2 \int_0^{\Theta_D/T} \frac{x dx}{e^x - 1} \right] \right\}, \quad (2)$$

where  $M$  is the mass of the Mössbauer nucleus,  $c$  is the speed of light,  $E_\gamma$  is the energy of the Mössbauer transition, and  $\Theta_D$  is the Debye temperature. Fig. 6 shows the temperature dependence of the spectral area  $A$  derived from the fits of the Mössbauer spectra in Fig. 3. The fit of the experimental dependence  $A(T)$  (Fig. 6) to Eq. (2) gives  $\Theta_D = 221(2)$  K. The value of  $\Theta_D$  found here is very close to the reported  $\Theta_D$  value of  $228(4)$  K for the nonsuperconducting compound  $\text{Tl}_{0.53}\text{K}_{0.47}\text{Fe}_{1.64}\text{Se}_2$  [30].

#### 4. Conclusions

The results of a  $^{57}\text{Fe}$  Mössbauer spectroscopy study of the new nonsuperconducting compound  $\text{TlFe}_{1.3}\text{Se}_2$  for temperatures between 4.4 and 373.2 K and in an external magnetic field of 90 kOe are reported. Evidence is provided for a possible phase separation into majority and minority magnetic phases. It is shown that these phases order antiferromagnetically with two different magnetic moments at 5.0 K of  $2.00(1)$  and  $1.40(2) \mu_B$ , and with the Néel temperature  $T_N = 324.5(6.3)$  K. The Debye temperature of the studied compound is found to be  $221(2)$  K.

#### Acknowledgments

This work was supported by the Natural Sciences and Engineering Research Council of Canada. Work at the Zhejiang University was supported by the National Science Foundation of China (Grants Nos. 10974175 and 109734005) and the National Basic Research Program of China (Grants Nos. 2011CBA00103, 2012CB821404, and 2009CB929104).

#### References

- [1] K. Klepp, H. Boller, *Monatsh. Chem.* 109 (1978) 1049.
- [2] L. Häggström, H.R. Verma, S. Bjarnan, R. Wäppling, *J. Solid State Chem.* 63 (1986) 401.
- [3] L. Häggström, A. Seidel, R. Berger, *Hyperfine Interact.* 54 (1990) 563.
- [4] L. Häggström, A. Seidel, R. Berger, *J. Magn. Magn. Mater.* 98 (1991) 37.
- [5] H.-H. Wen, S. Li, *Annu. Rev. Condens. Matter Phys.* 2 (2011) 121. and references therein.
- [6] D. Johrendt, H. Hosono, R.-D. Hoffmann, R. Pöttgen, *Z. Kristallogr.* 226 (2011) 435. and references therein.
- [7] G.R. Stewart, *Rev. Mod. Phys.* 83 (2011) 1589. and references therein.
- [8] J. Guo, S. Jin, G. Wang, S. Wang, K. Zhu, T. Zhou, M. He, X. Chen, *Phys. Rev. B* 82 (2010) 180520(R).
- [9] Y. Mizuguchi, H. Takeya, Y. Kawasaki, T. Ozaki, S. Tsuda, T. Yamaguchi, Y. Takano, *Appl. Phys. Lett.* 98 (2011) 042511.
- [10] A. Krzton-Maziopa, Z. Siermadini, E. Pomjakushina, V. Pomjakushina, M. Bendele, A. Amato, R. Khasanov, H. Luetkens, K. Coner, *J. Phys.: Condens. Matter* 23 (2011) 052203.
- [11] J.J. Ying, X.F. Wang, X.G. Luo, A.F. Wang, M. Zhang, Y.J. Yan, Z.J. Xiang, R.H. Liu, P. Cheng, G.J. Ye, X.H. Chen, *Phys. Rev. B* 83 (2011) 212502.

- [12] A.F. Wang, J.J. Ying, Y.J. Yan, R.H. Liu, X.G. Luo, Z.Y. Li, X.F. Wang, M. Zhang, G.J. Ye, P. Cheng, Z.J. Xiang, X.H. Chen, *Phys. Rev. B* 83 (2011) 060512(R).
- [13] H.-D. Wang, C.-H. Dong, Z.-J. Li, Q.-H. Mao, S.-S. Zhu, C.-M. Feng, H.Q. Yuan, M.-H. Fang, *Europhys. Lett.* 93 (2011) 47004.
- [14] M.-H. Fang, H.-D. Wang, C.-H. Dong, Z.-J. Li, C.-M. Feng, J. Chen, H.Q. Yuan, *Europhys. Lett.* 94 (2011) 27009.
- [15] M. Pfisterer, G. Nagorsen, *Z. Naturforsch. B* 35 (1980) 703.
- [16] P. Zavalij, W. Bao, X.F. Wang, J.J. Ying, X.H. Chen, D.M. Wang, J.B. He, X.Q. Wang, G.F. Chen, P.-Y. Hsieh, Q. Huang, M.A. Green, *Phys. Rev. B* 83 (2011) 132509.
- [17] F. Ye, S. Chi, W. Bao, X.F. Wang, J.J. Ying, X.H. Chen, H.D. Wang, C.H. Dong, M. Fang, *Phys. Rev. Lett.* 107 (2011) 137003.
- [18] J. Bacsá, A.Y. Ganin, Y. Takabayashi, K.E. Christensen, K. Prassides, M.J. Rosseinsky, J.B. Claridge, *Chem. Sci.* 2 (2011) 1054.
- [19] Z. Shermadini, A. Krzton-Maziopa, M. Bendele, R. Khasanov, H. Luetkens, K. Conder, E. Pomjakushina, S. Weyeneth, V. Pomjakushin, O. Bossen, A. Amato, *Phys. Rev. Lett.* 106 (2011) 117602.
- [20] R.H. Liu, X.G. Luo, M. Zhang, A.F. Wang, J.J. Ying, X.F. Wang, Y.J. Yan, Z.J. Xiang, P. Cheng, G.J. Ye, Z.Y. Li, X.H. Chen, *Europhys. Lett.* 94 (2011) 27008.
- [21] M. Wang, C. Fang, D.-X. Yao, G.T. Tan, L.W. Harriger, Y. Song, T. Netherton, C. Zhang, M. Wang, M.B. Stone, W. Tian, J. Hu, P. Dai, *Nat. Commun.* 2 (2011) 588.
- [22] W. Bao, Q.-Z. Huang, G.-F. Chen, M.A. Green, D.-M. Wang, J.-B. He, Y.-M. Qiu, *Chin. Phys. Lett.* 28 (2011) 086104.
- [23] Y.J. Yan, M. Zhang, A.F. Wang, J.J. Ying, Z.Y. Li, W. Qin, X.G. Luo, J.Q. Li, J. Hu, X.H. Chen, *Sci. Rep.* 2 (2012) 212.
- [24] V. Yu. Pomjakushin, D.V. Sheptyakov, E.V. Pomjakushina, A. Krzton-Maziopa, K. Conder, D. Chernyshov, V. Svitlyk, Z. Shermadini, *Phys. Rev. B* 83 (2011) 144410.
- [25] V. Yu. Pomjakushin, E.V. Pomjakushina, A. Krzton-Maziopa, K. Conder, Z. Shermadini, *J. Phys.: Condens. Matter* 23 (2011) 156003.
- [26] W. Bao, G.N. Li, Q. Huang, G.F. Chen, J.B. He, M.A. Green, Y. Qiu, D.M. Wang, J.L. Luo, M.M. Wu, *Chin. Phys. Lett.* 30 (2013) 027402.
- [27] Z.M. Stadnik, P. Wang, J. Żukrowski, H.-D. Wang, C.-H. Dong, M.-H. Fang, *J. Alloys Comp.* 549 (2013) 288, and references therein.
- [28] J.J. Ying, A.F. Wang, Z.J. Xiang, X.G. Luo, R.H. Liu, X.F. Wang, Y.J. Yan, M. Zhang, G.J. Ye, P. Cheng, X.H. Chen, e-print arXiv: 1012.2929.
- [29] B.C. Sales, M.A. McGuire, A.F. May, H. Cao, B.C. Chakoumakos, A.S. Sefat, *Phys. Rev. B* 83 (2011) 224510.
- [30] Z.M. Stadnik, P. Wang, J. Żukrowski, H.-D. Wang, C.-H. Dong, M.-H. Fang, *J. Phys.: Condens. Matter* 24 (2012) 245701.
- [31] H. Cao, C. Cantoni, A.F. May, M.A. McGuire, B.C. Chakoumakos, S.J. Pennycook, R. Custelcean, A.S. Sefat, B.C. Sales, *Phys. Rev. B* 85 (2012) 054515.
- [32] Certificate of Calibration, Iron Foil Mössbauer Standard, Natl. Bur. Stand. (U.S.) Circ. No. 1541, edited by J.P. Cali (U.S. GPO, Washington, DC, 1971).
- [33] B.F. Otterloo, Z.M. Stadnik, A.E.M. Swolfs, *Rev. Sci. Instrum.* 54 (1983) 1575.
- [34] N.N. Greenwood, T.C. Gibb, *Mössbauer Spectroscopy*, Chapman and Hall, London, 1971; P. Gütllich, E. Bill, A. Trautwein, *Mössbauer Spectroscopy and Transition Metal Chemistry*, Springer, Berlin, 2011.
- [35] S. Margulies, J.R. Ehrman, *Nucl. Instrum. Methods* 12 (1961) 131; G.K. Shenoy, J.M. Friedt, H. Maletta, S.L. Ruby, in: I.J. Gruverman, C.W. Seidel, D.K. Dieterly (Eds.), *Mössbauer Effect Methodology*, vol. 10, Plenum, New York, 1974, p. 277.
- [36] G. Martínez-Pinedo, P. Schwerdtfeger, E. Caurier, K. Langanke, W. Nazarewicz, T. Söhnel, *Phys. Rev. Lett.* 87 (2001) 062701.
- [37] H. Sabrowsky, M. Rosenberg, D. Welz, P. Deppe, W. Schäfer, *J. Magn. Magn. Mater.* 54–57 (1986) 1497.
- [38] L. Ma, G.F. Li, J. Dai, J.B. He, D.M. Wang, G.F. Chen, B. Normand, W. Yu, *Phys. Rev. B* 84 (2011) 220505(R).
- [39] A.M. Zhang, J.H. Xiao, Y.S. Li, J.B. He, D.M. Wang, G.F. Chen, B. Normand, Q.M. Zhang, T. Xiang, *Phys. Rev. B* 85 (2012) 214508.
- [40] P. Panissod, J. Durand, J.I. Budnik, *Nucl. Instrum. Meth.* 199 (1982) 99; P. Panissod, *Hyperfine Interact.* 24–26 (1985) 607; O. Eriksson, A. Svane, *J. Phys.: Condens. Matter* 1 (1989) 1589; S.M. Dubiel, *J. Alloys Comp.* 488 (2009) 18.
- [41] D. Welz, P. Deppe, W. Schaefer, H. Sabrowsky, M. Rosenberg, *J. Phys. Chem. Solids* 50 (1989) 297.
- [42] C.E. Johnson, *J. Phys. D* 29 (1996) 2266, and references therein.
- [43] T.E. Cranshaw, G. Longworth, in: G.J. Long (Ed.), *Mössbauer Spectroscopy Applied to Inorganic Chemistry*, vol. 1, Plenum, New York, 1984, p. 171, and references therein.
- [44] E.N. Kaufmann, R.H. Vianden, *Rev. Mod. Phys.* 51 (1979) 161, and references therein.
- [45] K. Nishiyama, F. Dimmling, Th. Kornrumpf, D. Riegel, *Phys. Rev. Lett.* 37 (1976) 357; J. Christiansen, P. Heubes, R. Keitel, W. Klinger, W. Loeffler, W. Sandner, W. Witthuhn, *Z. Phys. B* 24 (1976) 177; P. Jena, *Phys. Rev. Lett.* 36 (1976) 418.